PRL 115, 023201 (2015) PHYSICAL REVIEW LETTERS week ending 10 JULY 2015

Tuning Bimolecular Chemical Reactions by Electric Fields

Timur V. Tscherbul[1,2] and Roman V. Krems[2]
[1]Chemical Physics Theory Group, Department of Chemistry, and Center for Quantum Information and Quantum Control, University of Toronto, Toronto, Ontario M5S 3H6, Canada
[2]Department of Chemistry, University of British Columbia, Vancouver, British Columbia V6T 1Z1, Canada

(Received 12 August 2014; revised manuscript received 22 April 2015; published 6 July 2015)

We develop a theoretical method for solving the quantum mechanical reactive scattering problem in the presence of external fields based on a hyperspherical coordinate description of the reaction complex combined with the total angular momentum representation for collisions in external fields. The method allows us to obtain converged results for the chemical reaction $\mathrm{LiF} + \mathrm{H} \rightarrow \mathrm{Li} + \mathrm{HF}$ in an electric field. Our calculations demonstrate that, by inducing couplings between states of different total angular momenta, electric fields with magnitudes < 150 kV/cm give rise to resonant scattering and a significant modification of the total reaction probabilities, product state distributions, and the branching ratios for reactive versus inelastic scattering.

DOI: 10.1103/PhysRevLett.115.023201 PACS numbers: 34.50.Lf, 34.50.Cx

Tuning microscopic chemical reactions with external fields has long been an ultimate goal in chemical reaction dynamics [1]. This goal stimulated the development of quantum control schemes [2,3], which have been applied with spectacular results to unimolecular reactions. Attaining control over bimolecular reactions in a gas has proven to be a much bigger challenge due to the randomness of the rotational and translational motion of the reactants [4,5]. This randomness can be reduced by cooling molecules to low temperatures [4,6], enabling the detection of quantum resonance effects in cold reactions [7,8]. Recent experiments [9–11] demonstrated that chemical reactions in an ultracold gas of KRb molecules can be effectively suppressed by applying an electric field. While demonstrating that the randomness of the molecular motion can be harnessed, the control mechanism in Refs. [9,10] amounts to switching off reactive collisions by tunable long-range barriers, which prevent the reactants from approaching close enough to undergo chemical transformations.

In general, for chemical reactions to occur, molecules must approach each other at close range, where the interactions induced by external fields (typically ∼1 K in magnitude) must compete with strong intermolecular interactions (often > 1000 K) at short separations between the reactants. Since the external field-induced couplings are so small compared to intermolecular interactions, it is not clear if external fields can be used to steer chemical reactions. For example, the effects of external fields on the product state distributions and branching ratios for different reaction channels remain completely unknown. While the rates of low-temperature chemical reactions can be sensitive to scattering resonances [5,7,8], it is not known if the resonances capable of affecting the outcome of a chemical reaction can be induced by electric or magnetic fields with feasible strengths.

These questions stimulated the mounting number of experiments on chemical reaction dynamics in external fields [12]. Several quantum threshold models [13] and quantum defect theories [14,15] were proposed to describe the observations. While these models provide valuable insight into the effect of long-range interactions on ultracold reactions, with a single exception [16] they do not describe the reaction dynamics at short range and thus can be applied to model only the averaged quantities such as the total reaction rates. The detailed dynamics of chemical reactions is most accurately encoded in the state-to-state scattering S matrices, which can be obtained by quantum reactive scattering calculations. However, even in the absence of external fields, the quantum reactive scattering problem is challenging due to the presence of multiple reaction arrangements and the computational expense due to a large number of rovibrational states involved [17–20]. The presence of external fields further complicates the problem, making it necessary to consider the coupling between states with different total angular momenta of the reaction complex. As a consequence, a detailed microscopic understanding of how external fields influence the reaction mechanisms is still missing.

In this Letter, we report the first numerically exact quantum scattering calculation on a chemical reaction in an external field. Using a newly developed theoretical approach based on hyperspherical coordinates [17,19] combined with the total angular momentum representation for collisions in external fields [21,22], we show that the total cross sections and the nascent product state distribution of an atom-diatom reaction ($\mathrm{LiF} + \mathrm{H} \rightarrow \mathrm{Li} + \mathrm{HF}$) at low collision energies can be effectively controlled by laboratory-realizable dc electric fields via tunable reactive scattering resonances. This work suggests that a wide range of experimentally relevant problems previously considered intractable are now amenable to theoretical study, including the effects on low-temperature chemical dynamics of reactants' spin polarization [23], magnetic Feshbach resonances, and deviations from universality [24], and field-controlled near-resonant energy transfer [20,25].

We begin by outlining our quantum reactive scattering approach. For the three-atom reaction considered here, there are two reaction arrangements, Li + HF and H + LiF, that need to be considered simultaneously [26]. To do this, we use the Fock-Delves hyperspherical coordinates. Expressed in these coordinates, the Hamiltonian of the atom-molecule reaction complex in the presence of an external field is [17,19,20]

$$\hat{H} = \frac{-1}{2\mu\rho^5}\frac{\partial}{\partial\rho}\rho^5\frac{\partial}{\partial\rho} + \frac{(\hat{\boldsymbol{J}} - \hat{\boldsymbol{j}}_\alpha)^2}{2\mu\rho^2\cos^2\theta_\alpha} + V(\rho,\theta_\alpha,\gamma_\alpha) + \hat{H}_{\mathrm{mol},\alpha}, \tag{1}$$

where $\rho = (R_\alpha^2 + r_\alpha^2)^{1/2}$ is the hyperradius, θ_α and γ_α are the hyperangles defined by $\tan\theta_\alpha = r_\alpha/R_\alpha$, and $\cos\gamma_\alpha = (\boldsymbol{R}_\alpha \cdot \boldsymbol{r}_\alpha)/(R_\alpha r_\alpha)$, and $\boldsymbol{R}_\alpha$ and $\boldsymbol{r}_\alpha$ are mass-scaled Jacobi vectors in arrangement $\alpha = 1, 2, 3$ [17].

In Eq. (1), $\hat{\boldsymbol{J}}$ is the total angular momentum of the reaction complex and $\hat{\boldsymbol{j}}_\alpha$ is the rotational angular momentum of the diatomic molecule in arrangement α. The interaction of the reactants and products with the external field is included in the last term of Eq. (1). For reactions in a dc electric field, this term is [20]

$$\hat{H}_{\mathrm{mol},\alpha} = \frac{-1}{2\mu\rho^2\sin^2 2\theta_\alpha}\frac{\partial}{\partial\theta_\alpha}\sin^2 2\theta_\alpha\frac{\partial}{\partial\theta_\alpha} + \frac{\hat{j}_\alpha^2}{2\mu\rho^2\sin^2\theta_\alpha} + V_\alpha(\rho,\theta_\alpha) - \boldsymbol{d}_\alpha(\rho,\theta_\alpha)\cdot\boldsymbol{E}, \tag{2}$$

where $\boldsymbol{d}_\alpha$ is the electric dipole moment of the diatomic molecule in arrangement α and $\boldsymbol{E}$ is the electric field vector, which defines a space-fixed quantization axis. The wave function of the reaction complex is expanded in hyperspherical adiabatic surface functions

$$\Psi = \rho^{-5/2}\sum_i F_i(\rho)\Phi_i(\rho;\Omega), \tag{3}$$

where $\Phi_i(\Omega)$ are obtained by solving the adiabatic eigenvalue problem $\hat{H}_{\mathrm{ad}}\Phi_i(\Omega;\rho) = \epsilon_i(\rho)\Phi_i(\Omega;\rho)$, $\epsilon_i(\rho)$ are the adiabatic hyperspherical energies, and $\hat{H}_{\mathrm{ad}}$ is the adiabatic surface Hamiltonian obtained by subtracting the hyperradial kinetic energy from the full Hamiltonian in Eq. (1) [17,19,20]. To solve the eigenvalue problem, we expand the surface functions as [19,21,22]

$$\Phi_i(\rho;\Omega) = \sum_{\alpha,v,j,J,k,\eta} W_{\alpha vjJk\eta,i}|\alpha vjJk\eta\rangle, \tag{4}$$

where $|\alpha vjJk\eta\rangle = |JMk\eta\rangle 2\chi_{\alpha vj}(\theta_\alpha;\rho)/(\sin 2\theta_\alpha)$ and $\chi_{\alpha vj}(\theta_\alpha;\rho)$ are the primitive Fock-Delves basis functions, which diagonalize the Hamiltonian in Eq. (2) at zero field [20]. The states $|JMk\eta\rangle$ are the angular basis functions

$$|JMk\eta\rangle = N_k[|JMk\rangle|jk\rangle + \eta(-1)^J|JM-k\rangle|j-k\rangle] \tag{5}$$

composed of the spherical harmonics $|jk\rangle = \sqrt{2\pi}Y_{jk}(\theta_\alpha,0)$ and the symmetric top eigenfunctions $|JMk\rangle$, where η is the inversion parity, M and k are the projections of J on the space-fixed and body-fixed quantization axes, respectively [17], and $N_k = [2(1+\delta_{k0})]^{-1/2}$. The basis (4) is key to the efficiency of the method we propose here. In an external field, J and η are not conserved but the matrix of the field-induced interaction in the basis (4) is tridiagonal in J and thus only a limited number of J states is generally required for a fully converged calculation [22]. This offers a great computational advantage over the previously proposed approach [20], which disregards the total angular momentum of the reaction complex. All calculations are performed using the quantum reactive scattering program ABC [18], extensively modified to incorporate the effects of electric fields (see the Supplemental Material [28]).

We now apply this methodology to study the effects of electric fields on the chemical reaction LiF + H→ HF + Li. The choice of the reaction is motivated by the large permanent electric dipole moment of LiF ($d = 6.3$ D), thus leading one to expect large electric field effects in the entrance reaction channel, but not in the outgoing channels [20]. In addition, the inverse reaction Li + HF → LiF + H has been the focus of numerous theoretical and experimental studies [27,32–34]. An experimental study of its low-temperature dynamics is in progress using a rotating nozzle source of HF molecules combined with a magneto-optical trap for Li atoms [34]. The LiF + H reaction can similarly be studied using a cold ensemble of H atoms in a magnetic trap [35,36] combined with a slow beam of LiF molecules [37,38]. While such an experiment can be challenging to realize, we note that due to the low reduced mass of the reactants, the few partial wave regime desirable for the observation of the effects discussed below can be reached with only moderate cooling of the reactants ($T \sim 1$ K). Collisions at such temperatures can also be probed by the merged beam techniques [7,8].

To describe the atom-molecule interaction $V(\rho,\theta_\alpha,\gamma_\alpha)$ in the LiHF reaction complex, we use an accurate *ab initio* potential energy surface [33] previously employed in field-free reaction rate calculations at low temperatures [27]. Figure 1 illustrates the key features of the potential energy surface. The reaction proceeds through a transition state that has a bent configuration and the barrier height is 518 cm^{-1} relative to the bottom of the LiF potential well [33]. The chemical reaction LiF($v = 1, j = 0$) + H → HF($v = 0, j = 0$) + Li is slightly exoergic ($\Delta E = 0.1$ eV), and a total of six HF rotational states are energetically accessible at zero collision energy.

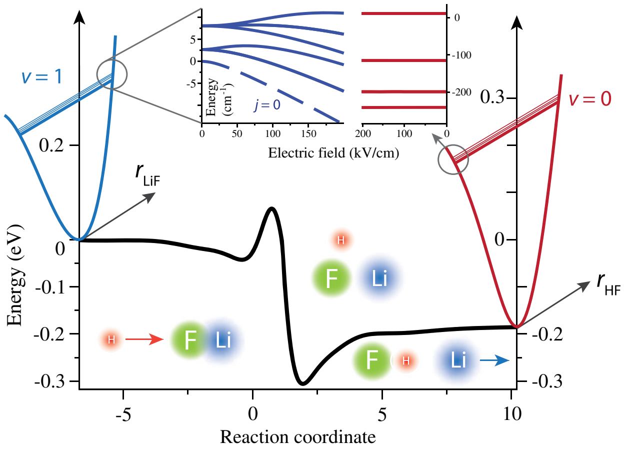

FIG. 1 (color online). Schematic diagram of the LiF + H → HF + Li chemical reaction showing (1) the minimum energy path along the reaction coordinate $s = r_{\mathrm{LiF}} - r_{\mathrm{HF}}$, (2) vibrational potential energy curves of the reactants and products, and (3) the Stark structure of LiF and HF (not to scale).

Figure 2 shows the total cross section for HF production in the chemical reaction of LiF($v = 1, j = 0$) with H as a function of electric field for a collision energy of 0.01 cm^{-1}. At low temperatures, the reaction occurs by the tunneling of a heavy F atom [27] and hence the reaction cross section is small. An applied electric field causes modulation of the reaction cross section below 100 kV/cm. The most remarkable feature apparent in Fig. 2 is a pronounced resonance triplet at $E \sim 125$ kV/cm (peaks A, B, and C). The central resonance B corresponds to an electric-field-induced enhancement of chemical reactivity by a factor of 42. Resonances A and C have widths of 0.10 and 0.18 kV/cm, while resonance B is at least 10 times narrower ($\Gamma \leq 0.02$ kV/cm). To investigate the origin of these resonances, we computed the electric field dependence of the van der Waals (vdW) bound states in the entrance reaction channel H ⋯ LiF. We confirmed that (1) the resonances can be assigned to the bound states of the H ⋯ LiF vdW complex, and (2) the resonances disappear if exit-channel rovibrational states are omitted from the basis set. The resonances shown in Fig. 2 are thus similar to the vdW resonances [27,39–43] that decay via a remarkable “prereaction” mechanism involving tunneling through the reaction barrier, even though the resonance wave function is localized in the entrance reaction channel [27]. Although the resonances acquire finite width due to coupling to the exit reaction channel, they are sensitive to the electric field precisely because they are located in the entrance reaction channel, where the reactive system is significantly more polar.

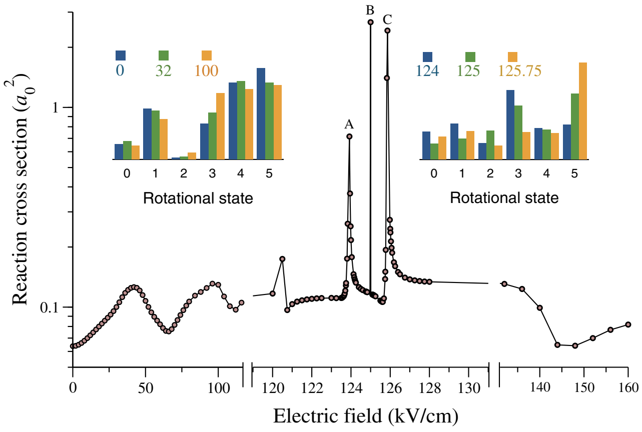

FIG. 2 (color online). Electric field dependence of the total cross section for the reaction LiF + H → HF + Li. The insets show the nascent rotational state distributions of HF molecules produced in the reaction as a function of the final rotational state j' at electric field strengths of 0, 32, and 100 kV/cm (left) and 124, 125, and 125.75 kV/cm (right). Note the dramatic change in the shape of the distribution near the resonance electric field (right inset). All calculations were performed in the Wigner s-wave regime ($E_C = 0.01$ cm^{-1}), where no resonances are present in the reaction cross sections as a function of collision energy [27].

We next consider another important observable property of a chemical reaction, the nascent product state distribution $\sigma_{\alpha v j \to \alpha' v' j'} / \sum_{\alpha' v' j'} \sigma_{\alpha v j \to \alpha' v' j'}$, where $\sigma_{\alpha v j \to \alpha' v' j'}$ is the cross section for the $\alpha v j \to \alpha' v' j'$ reaction process. This distribution quantifies the amount of internal energy with which the reaction products form. Figure 2 shows that low-to-moderate electric fields modify the rotational distributions of HF by changing the relative populations of $j' = 3$ and $j' = 5$. As shown below, this effect occurs due to the emergence of new chemical reaction pathways forbidden at zero fields by total angular momentum conservation.

At $E \sim 125$–127 kV/cm corresponding to the field-induced resonances A, B, and C, the shape of the nascent product state distribution changes dramatically. Away from the resonances, we observe a “hot” HF product distribution that peaks at $j' = 5$ and falls off gradually with decreasing j'. On resonance A, the distribution develops a pronounced peak at $j' = 3$ and behaves nonmonotonically as a function of j', indicating a dramatic change in the reaction mechanism across a narrow interval of electric fields. On resonance B, the HF products are formed with a more even distribution over rotational energy levels, with $j' =$ 2–5 all substantially populated. As the electric field is tuned across resonance C, a unimodal distribution develops centered at $j' = 5$. The preferential population of high j states on resonances A–C can be explained by a relatively high degree of rotational excitation ($j = 4$) of the LiF fragment in the vdW complex H ⋯ LiF that gives rise to the resonance states. A more even product state distribution on resonance B results from its longer lifetime, which allows the rotational degrees of freedom to equilibrate more efficiently.

In order to gain insight into the mechanism of electric field control of reaction cross sections and product state

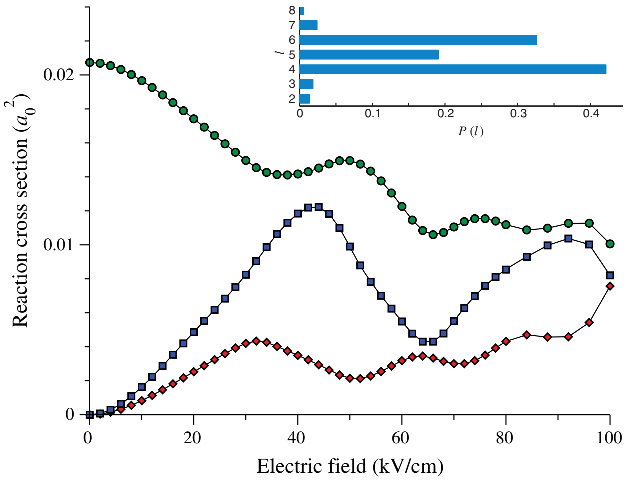

FIG. 3 (color online). Partial wave contributions to the cross section for the LiF$(v = 1, j = 0) \to$ HF$(v' = 0, j' = 5)$ reactive transition as functions of an applied electric field. This transition dominates the total reaction cross section in the range of electric fields close to the resonance triplet (see Fig. 2). Circles: J-conserving transition $\ell = 0 \to \ell' = 5$. Squares and diamonds: J-changing transitions $\ell = 0 \to \ell' = 4, 6$. The inset shows the individual partial wave contribution to the $j = 0 \to j' = 5$ reactive cross section on resonance at $E = 125$ kV/cm. A total of four J states ($J = 0$–3) were included in scattering calculations [28].

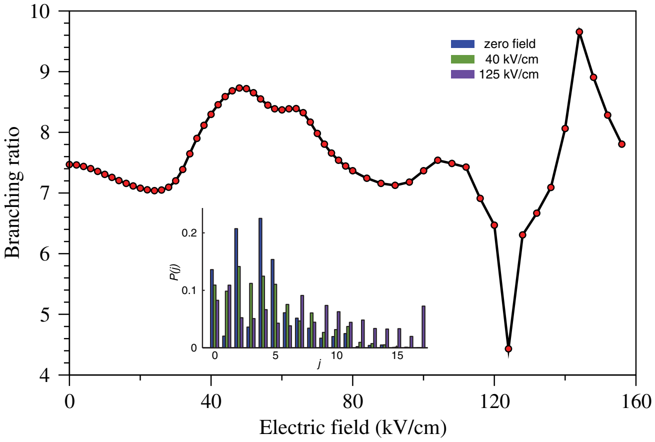

FIG. 4 (color online). The branching ratio for inelastic to reactive cross sections as a function of electric field. The inset shows rotational product state distributions for vibrational relaxation in nonreactive LiF$(v = 1, j = 0) +$ H collisions.

distributions, we focus on the dominant reactive transition $j = 0 \to j' = 5$. In Fig. 3, we plot the contributions of the different partial wave transitions $j = 0, \ell = 0 \to j', \ell'$ as a function of the electric field strength. Since the total angular momentum of the collision complex $\boldsymbol{J} = \boldsymbol{j} + \boldsymbol{\ell} = \boldsymbol{j}' + \boldsymbol{\ell}'$ is conserved at zero field, and $j = \ell = 0$ in the entrance reaction channel (assuming s-wave scattering), it follows that $j' + \ell' = 0$ and hence $\ell' = j'$. Thus, only the $\ell' = 5$ partial wave contribution is allowed at zero field. The line with circles in Fig. 3 confirms this. An external field induces couplings between the adjacent J states [20,22]. As a result, the off-diagonal, J-changing transitions $j = 0$, $\ell = 0 \to j', \ell' = j' \pm 1$ become allowed, as illustrated in Fig. 3. While these J-changing transitions play a minor role at low fields, they become dominant at fields above 100 kV/cm. As shown in the inset of Fig. 3, the J-changing transitions $\ell = 0 \to \ell' = 4, 6$ make up more than 70% of the reaction cross section at $E = 125$ kV/cm (on resonance B). We therefore refer to resonance B as the electric-field-induced resonance.

While the electric-field-induced resonances can greatly enhance the reaction cross section, the excess vibrational energy of the LiF$(v = 1, j = 0)$ reactants can also be converted into translational energy via nonreactive collisions leading to vibrational relaxation. To explore the possibility of controlling the relative efficiency of these competing pathways, we plot in Fig. 4 the electric field dependence of the ratio of cross sections for vibrational relaxation and reactive scattering. At low fields, the branching ratio varies insignificantly, and vibrational relaxation remains as efficient as it is at zero field. Near the electric-field-induced resonance, however, the branching ratio drops to 4 before rising back to 10.

The electric field dependence of the LiF$(v = 0, j')$ product distribution following vibrational relaxation in LiF$(v = 1, j = 0) +$ H collisions is plotted in the inset of Fig. 4 as a function of j'. We observe strong variation of the distributions even at low electric fields. A moderate field of 40 kV/cm broadens the distribution significantly, populating higher j' states. We attribute this effect to the field-induced hybridization of LiF rotational states in the $v = 0$ manifold, which modifies the anisotropic part of the LiF-H interaction potential and changes the relative populations of final rotational states. At resonance B, the rotational distribution becomes extremely broad and multimodal. While transitions to high-j states are suppressed at low-to-moderate electric fields, they become allowed at $E = 125$ kV/cm, signaling a profound change in the mechanism of rovibrational energy transfer near electric-field-induced scattering resonances. This mechanism is different from that explored in previous work on near-resonant energy transfer in cold collisions [44] as the energy gaps between the rovibrational levels of the reactants and products remain large (>20 cm^{-1}) in the range of electric fields explored in this work.

In conclusion, we have introduced a theoretical method for solving the quantum reactive scattering problem in the presence of an external field based on a hyperspherical coordinate formalism [17–19] combined with the total angular momentum representation for molecular collisions in external fields [21,22]. The method is much more efficient than the previous rigorous approach [20] and makes it possible to obtain numerically converged results for a three-dimensional atom-diatom chemical reaction in a dc electric field. The efficiency can be further enhanced by transforming away the off-diagonal J blocks, or by matching to quantum defect solutions [16]. Our methodology can be applied to any abstraction atom-diatom chemical reaction in magnetic, dc electric, and off-resonant microwave and laser fields. It can also be extended to calculations on barrierless insertion chemical reactions by changing the hyperspherical part of the treatment to the Smith-Whitten coordinates [45]. The main idea of combining the field-free reactive scattering problems formulated in the J representation and including field-dependent couplings between different J states would still apply.

This work was supported by NSERC of Canada. We are grateful to Dajiang Ding and Sylvain Korzennik for their expert assistance with high-performance computing.

[1] R. N. Zare, Science **279**, 1875 (1998).

[2] M. Shapiro and P. Brumer, *Quantum Control of Molecular Processes* (Wiley-VCH, Weinheim, 2012).

[3] S. A. Rice and M. Zhao, *Optical Control of Molecular Dynamics* (Wiley, New York, 2000).

[4] R. V. Krems, Phys. Chem. Chem. Phys. **10**, 4079 (2008).

[5] D. Herschbach, Faraday Discuss. **142**, 9 (2009).

[6] L. D. Carr, D. DeMille, R. V. Krems, and J. Ye, New J. Phys. **11**, 055049 (2009).

[7] A. B. Henson, S. Gersten, Y. Shagam, J. Narevicius, and E. Narevicius, Science **338**, 234 (2012).

[8] E. Lavert-Ofir, Y. Shagam, A. B. Henson, S. Gersten, J. Kłos, P. S. Żuchowski, J. Narevicius, and E. Narevicius, Nat. Chem. **6**, 332 (2014).

[9] K.-K. Ni, S. Ospelkaus, D. Wang, G. Quéméner, B. Neyenhuis, M. H. G. de Miranda, J. L. Bohn, J. Ye, and D. S. Jin, Nature (London) **464**, 1324 (2010).

[10] M. H. G. de Miranda, A. Chotia, B. Neyenhuis, D. Wang, G. Quéméner, S. Ospelkaus, J. L. Bohn, J. Ye, and D. S. Jin, Nat. Phys. **7**, 502 (2011).

[11] G. Quéméner and P. S. Julienne, Chem. Rev. **112**, 4949 (2012).

[12] B. K. Stuhl, M. T. Hummon, and J. Ye, Annu. Rev. Phys. Chem. **65**, 501 (2014).

[13] G. Quéméner and J. L. Bohn, Phys. Rev. A **81**, 022702 (2010).

[14] Z. Idziaszek and P. S. Julienne, Phys. Rev. Lett. **104**, 113202 (2010).

[15] B. Gao, Phys. Rev. Lett. **105**, 263203 (2010).

[16] J. Hazra, B. P. Ruzic, J. L. Bohn, and N. Balakrishnan, Phys. Rev. A **90**, 062703 (2014).

[17] R. T. Pack and G. A. Parker, J. Chem. Phys. **87**, 3888 (1987).

[18] D. Skouteris, J. F. Castillo, and D. E. Manolopoulos, Comput. Phys. Commun. **133**, 128 (2000).

[19] G. C. Schatz, Chem. Phys. Lett. **150**, 92 (1988).

[20] T. V. Tscherbul and R. V. Krems, J. Chem. Phys. **129**, 034112 (2008).

[21] T. V. Tscherbul and A. Dalgarno, J. Chem. Phys. **133**, 184104 (2010).

[22] T. V. Tscherbul, Phys. Rev. A **85**, 052710 (2012).

[23] V. Singh, K. S. Hardman, N. Tariq, M.-J. Lu, A. Ellis, M. J. Morrison, and J. D. Weinstein, Phys. Rev. Lett. **108**, 203201 (2012).

[24] T. T. Wang, M.-S. Heo, T. M. Rvachov, D. A. Cotta, and W. Ketterle, Phys. Rev. Lett. **110**, 173203 (2013).

[25] E. R. Meyer and J. L. Bohn, Phys. Rev. A **82**, 042707 (2010).

[26] The F + LiH channel lies 3 eV above the reactants' threshold LiF$(v = 1, j = 0)$ and can thus be safely excluded from low-energy scattering calculations [27].

[27] P. F. Weck and N. Balakrishnan, J. Chem. Phys. **122**, 234310 (2005).

[28] See Supplemental Material at http://link.aps.org/supplemental/10.1103/PhysRevLett.115.023201, which includes Refs. [29–31], for details of reactive scattering calculations and convergence tests.

[29] D. E. Manolopoulos, J. Chem. Phys. **85**, 6425 (1986).

[30] R. V. Krems and A. Dalgarno, J. Chem. Phys. **120**, 2296 (2004).

[31] T. V. Tscherbul and R. V. Krems (to be published).

[32] S. C. Althorpe and D. Clary, Annu. Rev. Phys. Chem. **54**, 493 (2003).

[33] A. Aguado, M. Paniagua, C. Sanz, and O. Roncero, J. Chem. Phys. **119**, 10088 (2003).

[34] R. Bobbenkamp, H. Loesch, M. Mudrich, and F. Stienkemeier, J. Chem. Phys. **135**, 204306 (2011).

[35] H. F. Hess, G. P. Kochanski, J. M. Doyle, N. Masuhara, D. Kleppner, and T. J. Greytak, Phys. Rev. Lett. **59**, 672 (1987).

[36] A. W. Wiederkehr, S. D. Hogan, B. Lambillotte, M. Andrist, H. Schmutz, J. Agner, Y. Salathé, and F. Merkt, Phys. Rev. A **81**, 021402(R) (2010).

[37] J. E. van den Berg, S. C. Mathavan, C. Meinema, J. Nauta, T. H. Nijbroek, K. Jungmann, H. L. Bethlem, and S. Hoekstra, J. Mol. Spectrosc. **300**, 22 (2014).

[38] N. R. Hutzler, H.-I. Lu, and J. M. Doyle, Chem. Rev. **112**, 4803 (2012).

[39] T. Xie, D. Wang, J. M. Bowman, and D. E. Manolopoulos, J. Chem. Phys. **116**, 7461 (2002).

[40] V. Aquilanti, S. Cavalli, A. Simoni, A. Aguilar, J. M. Lucas, and D. De Fazio, J. Chem. Phys. **121**, 11675 (2004).

[41] V. Aquilanti, S. Cavalli, D. De Fazio, A. Simoni, and T. V. Tscherbul, J. Chem. Phys. **123**, 054314 (2005).

[42] K. Takahashi, M. Y. Hayes, and R. T. Skodje, J. Chem. Phys. **138**, 024309 (2013).

[43] M. L. González-Martínez and J. M. Hutson, Phys. Rev. A **75**, 022702 (2007).

[44] R. C. Forrey, N. Balakrishnan, A. Dalgarno, M. R. Haggerty, and E. J. Heller, Phys. Rev. Lett. **82**, 2657 (1999).

[45] R. C. Whitten and F. T. Smith, J. Math. Phys. (N.Y.) **9**, 1103 (1968).